

Nonlinear oscillations and rotations of a liquid droplet

Tadashi Watanabe

watanabe.tadashi66@jaea.go.jp

Abstract—Nonlinear oscillations and rotations of a liquid droplet are simulated numerically by solving the Navier-Stokes equations using the level set method. Mass conservation of droplet is especially taken into consideration for calculations of the level set function. The nonlinear effects of oscillation amplitude and rotation rate on oscillation frequency, which are known as the frequency shift, are shown quantitatively by comparing with theoretical predictions. It is shown for the normalized amplitude and the rotation rate smaller than 0.2 that the simulated frequency shifts are in good agreement with the theoretical predictions and the effects of viscosity and surface tension on the frequency shift are negligibly small.

Keywords— Level set method, Mass conservation, Navier-Stokes equation, Nonlinear droplet dynamics.

I. INTRODUCTION

A levitated liquid droplet is used to measure material properties of molten metal at high temperature, since the levitated droplet is not in contact with a container, and the effect of container wall is eliminated for precise measurement [1-3]. Properties of surfactant solutions [4] and molten silicon [5] are also measured using the levitated liquid droplet. Viscosity and surface tension are, respectively, obtained from the damping and the frequency of shape oscillations of the droplet. The relation between material properties and oscillation parameters is based on the linear theory [6], and small-amplitude oscillations are necessary. Large-amplitude oscillations are, however, desirable from the viewpoint of measurement. The effect of amplitude is inevitable for the measurement even for small-amplitude oscillations.

It has been shown experimentally [7,8] and numerically [9-12] that the frequency of drop-shape oscillations decreased with increasing amplitude. The effect of amplitude on the oscillation frequency has also been discussed theoretically [13]. Second order small deviations were taken into account for the linearized solution of the Lagrange equation, and the oscillation frequency was shown to decrease as the amplitude increased. On the other hand, the effect of rotation on the oscillation frequency has been discussed theoretically [14]. The force balance at the droplet surface between the surface tension and the pressure difference across the interface was considered. The dynamic pressure due to the first order effect of rotation was taken into account together with the distortions of the interface.

In contrast to the effect of amplitude, the oscillation frequency increased with increasing rotation. Although the nonlinear effects of oscillation amplitude and rotation were shown by these theoretical studies, quantitative estimation is not enough since the theoretical approach assumed lower-order effects. Numerical simulations to study the effects of amplitude and rotation on oscillation frequency have been performed, and the nonlinear effects were shown to be overestimated by theoretical predictions [15]. Quantitative treatment was, however, not so strict and the effects of viscosity and surface tension were not discussed, though the flow fields in and around the droplet were shown [15].

In this study, numerical simulations of oscillations and rotations of a liquid droplet are performed to study the nonlinear behavior of droplet quantitatively. Three-dimensional Navier-Stokes equations are solved using the level set method [16]. The level set method has been applied for simulations of moving interfaces and discontinuities in a wide variety of problems including material science [17,18]. The level set function, which is the distance function from the droplet surface, is calculated by solving the transport equation to obtain the surface position correctly. Mass conservation of the droplet is especially taken into consideration in the calculation of the level set function in the following. Nonlinear effects of oscillations and rotations are discussed in terms of the oscillation frequency, and the effects of viscosity and surface tension are clarified.

II. NUMERICAL METHOD

A. Governing Equations

Governing equations for the droplet motion are the equation of continuity and the incompressible Navier-Stokes equation including the effect of surface tension [16]:

$$\nabla \cdot \mathbf{u} = 0, \quad (1)$$

and

$$\rho \frac{D\mathbf{u}}{Dt} = -\nabla p + \nabla \cdot (2\mu\mathbf{D}) - \mathbf{F}_s, \quad (2)$$

where ρ , \mathbf{u} , p and μ , respectively, are the density, the velocity, the pressure and the viscosity, \mathbf{D} is the viscous stress tensor, and \mathbf{F}_s is a body force due to the surface tension. External force

fields such as the gravity are not simulated in this study. The surface tension force is given by

$$\mathbf{F}_s = \sigma \kappa \delta \nabla \phi \quad , \quad (3)$$

where σ , κ , δ and ϕ are the surface tension, the curvature of the interface, the Dirac delta function and the level set function, respectively. The level set function is a distance function defined as the normal distance from the interface: $\phi=0$ at the interface, $\phi<0$ in the liquid region, and $\phi>0$ in the gas region. The curvature of the interface is expressed in terms of ϕ :

$$\kappa = \nabla \cdot \left(\frac{\nabla \phi}{|\nabla \phi|} \right) \quad . \quad (4)$$

The density and viscosity are, respectively, given by

$$\rho = \rho_l + (\rho_g - \rho_l)H \quad , \quad (5)$$

and

$$\mu = \mu_l + (\mu_g - \mu_l)H \quad , \quad (6)$$

where the subscripts g and l indicate gas and liquid phases, respectively. In Eqs. (5) and (6), H is the Heaviside-like function defined by

$$H = \begin{cases} 0 & (\phi < -\varepsilon) \\ \frac{1}{2} \left[1 + \frac{\phi}{\varepsilon} + \frac{1}{\pi} \sin\left(\frac{\pi\phi}{\varepsilon}\right) \right] & (-\varepsilon \leq \phi \leq \varepsilon) \\ 1 & (\varepsilon < \phi) \end{cases} \quad , \quad (7)$$

where ε is a small positive constant for which $|\nabla \phi|=1$ for $|\phi| \leq \varepsilon$. The evolution of ϕ is given by

$$\frac{\partial \phi}{\partial t} + \mathbf{u} \cdot \nabla \phi = 0 \quad . \quad (8)$$

In order to maintain the level set function as a distance function, reinitialization of the level set function is proposed by solving the following equation [16]:

$$\frac{\partial \phi}{\partial \tau} = \text{sign}(\phi_0)(1 - |\nabla \phi|) \quad , \quad (9)$$

where τ is an artificial time, and $\text{sign}(\phi_0)$ indicates the sign of the level set function at the beginning of the reinitialization procedure defined by

$$\text{sign}(\phi_0) = \begin{cases} -1 & (\phi_0 < 0) \\ 0 & (\phi_0 = 0) \\ 1 & (\phi_0 > 0) \end{cases} \quad , \quad (10)$$

The level set function becomes a distance function in the steady-state solution of Eq. (9).

Variables are nondimensionalized using liquid properties and characteristic values: $\mathbf{x}'=\mathbf{x}/L$, $\mathbf{u}'=\mathbf{u}/U$, $t'=t/(L/U)$, $\tau'=\tau/(L/U)$, $p'=p/(\rho_l U^2)$, $\rho'=\rho/\rho_l$, $\mu'=\mu/\mu_l$, $\phi'=\phi/L$ where the primes denote dimensionless variables, and L and U are representative length and velocity, respectively. Two parameters appear in the nondimensional Navier-Stokes equation: the Reynolds number, $\rho_l L U / \mu_l$, corresponding to the viscosity, and the Weber number, $\rho_l L U^2 / \sigma$, corresponding to the surface tension.

B. Numerical Procedure

The finite difference method is used to solve the governing equations. The staggered mesh is used for spatial discretization of velocities. The convection terms are discretized using the second order upwind scheme and other terms by the second order central difference scheme. Time integration is performed by the second order Adams-Bashforth method. The SMAC method is used to obtain pressure and velocities [19]. The pressure Poisson equation is solved using the Bi-CGSTAB method. The domain decomposition technique is applied and the message passing interface (MPI) library is used for parallel computations [20,26].

The smoothed sign function proposed for numerical treatment of reinitialization [21] is used for Eq. (10);

$$\text{sign}(\phi) = \frac{\phi}{\sqrt{\phi^2 + h^2}} \quad , \quad (11)$$

where h is the spatial increment in the finite difference method for solving the governing equations. A smoothed version of the sign function was also used in [16]. Smoothing of the sign function might be necessary for calculations of interface motion with a large density ratio, since the density ratio of 1000 was simulated in [16] and [21], while the Boussinesq approximation was used and smoothing was not mentioned in [22].

In this study, mass conservation is especially taken into consideration to simulate nonlinear behavior of the droplet quantitatively. It has been reported that the mass conservation was not maintained in general with the above reinitialization procedure for the level set function, and another reinitialization procedure solving the following equation was proposed [22];

$$\frac{\partial \phi}{\partial \tau} = (A_0 - A)(P - \kappa) |\nabla \phi| \quad , \quad (12)$$

where A_0 denotes the total mass for the initial condition and A denotes the total mass corresponding to the level set function. P is a positive constant for stabilization, and 1.0 was used in [22]. The effect of Eq. (12) is compared with that of Eq. (9) in the following, and the reinitialization scheme to assure the mass conservation of the liquid droplet is proposed, since the oscillation frequency is much affected by the mass of the droplet.

C. Numerical Conditions

Free-decay oscillations of the droplet shape along the vertical axis are studied by changing the amplitude of the initial deformation and the rotation rate. A droplet with the average radius of 1.0 is placed in the centre of the rectangular simulation region, and the density ratio, ρ_g / ρ_l , and the viscosity ratio, μ_g / μ_l , are both fixed at 0.01. The Reynolds number and the Weber number varied from 200 to 400 and from 10 to 30, respectively, so that the effect of the liquid properties on the oscillation frequency is shown.

For simulations to study the effect of amplitude, the initial deformation is given by the Legendre polynomial of order 2 for the oscillations with no rotation. The position of the droplet surface, r , is thus given by

$$r(\vartheta) = r_0 \{1 + \Delta r(3 \cos^2 \vartheta - 1)/2\}, \quad (13)$$

where θ is the angle between the vertical axis and the line through the origin and the surface, and r_0 and Δr are the average radius and the amplitude, respectively. The range of the amplitude is from 0.02 to 0.74. For simulations to study the effect of rotation, the initial rotation is imposed as a rigid rotation with a constant angular velocity around the vertical axis. The initial shape is given as the rotating ellipsoid with the vertical radius determined from the rotation of initially-spherical droplets, and the initial amplitude is fixed at 0.02 of the vertical radius. The effect of rotation was shown in [15] with similar conditions, but the spherical shape was used as the initial shape of rotating droplet. The oscillation amplitude thus became large as the rotation rate increased, and the effect of amplitude was included largely in the numerical results in [15]. The ellipsoidal shape is thus used here as the initial shape to eliminate the amplitude effect on the rotating droplet. The range of the rotation rate is from 0 to 0.7. Periodic boundary conditions are applied at all the boundaries of the simulation region.

The effects of region size, nodding and time step size on simulation results have been examined and reported beforehand [15], and are not shown here. The number of calculation nodes in three-dimensional space was determined so as to eliminate the size effect: 100x100x100 for the amplitude smaller than 0.38, 120x120x120 for the amplitude from 0.47 to 0.56, and 140x140x140 for the amplitude larger than 0.65. The spatial increment was 0.03 in all directions. The time step size was determined so as to satisfy the CFL conditions due to surface tension and viscous terms [21]. The Courant number was chosen to be 0.5 and the time step size Δt used in the following simulations was 0.0023 - 0.0040.

The positive constant in Eq. (12) was set equal to 1.0 in the following as was the case in [22]. In our simulations, κ was close to 1.0. Then, assuming a small deviation $\Delta\phi$ from the zero level set, the order of magnitude of the right hand side was $(\Delta\phi)^2$ for Eq. (12) while $\Delta\phi$ for Eq. (9). Larger time step size $\Delta\tau$ was thus necessary for Eq. (12), and $\Delta\tau$ in Eqs. (9) and (12) were set equal to $0.1\Delta t$ and $1.0\Delta t$, respectively, after some trial calculations. The order of magnitude could be the same by

scaling the term $(A_0 - A)$ using the interfacial area, for instance. In this case, the mass correction might be involved in the distance correction by adding a correction term similar to the right hand side of Eq. (12) to Eq. (9) [23]. The convergence criteria for the relative error of ϕ in Eqs. (9) and (12) were both 3.0×10^{-5} , and actually one iteration was necessary for both procedures.

III. RESULTS AND DISCUSSION

A. Mass Conservation

The mass conservation of the level set method is evaluated here for simulating simple shape oscillations. Figure 1 shows the time history of the vertical radius with different reinitialization schemes. Four cases are shown: the case with distance and mass corrections using Eqs. (9) and (12), the case with distance correction using Eq. (9), the case with mass correction using Eq. (12), and the case with no correction. The Reynolds number and the Weber number are, respectively, 200 and 20, and the initial amplitude and the rotation rate are 0.02 and 0.0, respectively. It is shown in Fig. 1 that all cases are almost the same in the early stage of the transient. The cases with mass correction and no correction, however, become unstable and show anomalous behavior. It has been reported [22] that merging bubbles were simulated without any problem using the level set method with no reinitialization schemes. The fourth order numerical schemes in time and space were, however, used with a fine mesh system in [22]. It is found in Fig. 1 that the distance correction using Eq. (9) is necessary for simulations of droplet oscillations under the numerical conditions in the present study. The distance correction is, thus, always performed in the following simulations regardless of the mass correction.

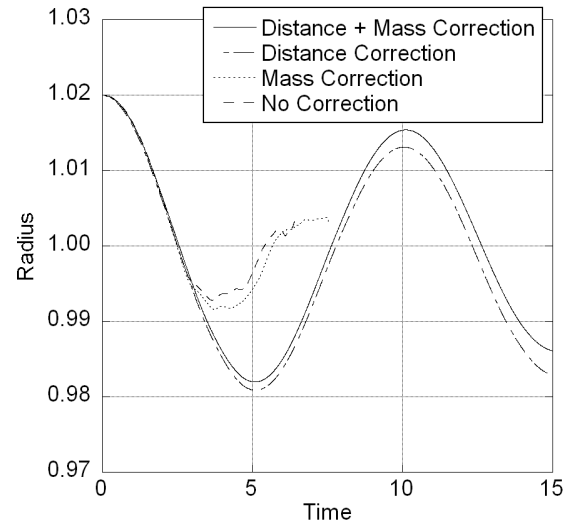


Fig. 1 Effects of distance and mass corrections on droplet radius.

Two cases with distance correction shown in Fig. 1 show qualitatively the same oscillation behavior in time. The droplet radius is, however, seen to be small for the case with distance correction, in other words, for the case with no mass correction. The time history of the droplet radius is shown for longer time in

Fig. 2 with different initial amplitude Δr to see the effect of amplitude on the difference between the cases with and without mass correction. It is seen for both cases with different amplitude that peak positions become small for the cases without mass correction. It indicates that the droplet radius becomes small without mass correction regardless of the amplitude. Furthermore, it is clear for the case with $\Delta r=0.11$ that the oscillation frequency is larger for the case without mass correction.

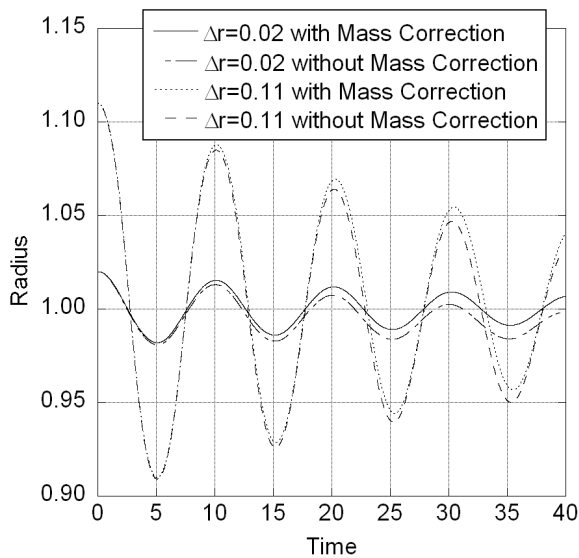


Fig. 2 Effects of mass correction and amplitude on droplet radius.

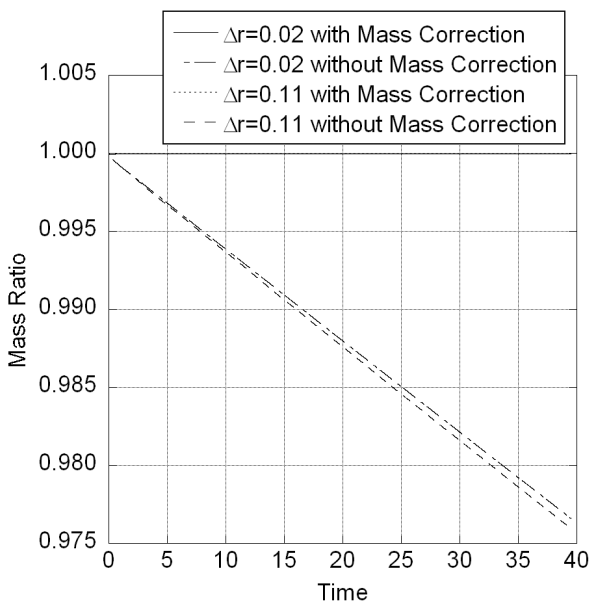


Fig. 3 Effects of mass correction and amplitude on mass ratio.

In order to see clearly the effect of mass correction, the time history of the mass ratio, which is defined as the ratio of the total mass to the initial mass in the simulation region, is shown in Fig. 3 corresponding to Fig. 2. The mass ratio decreases almost

linearly for the cases without mass correction, while it is kept at about 1.0 for the cases with mass correction. It is found that the droplet mass is lost in time if the mass correction is not taken into consideration. The loss of mass was also observed in [22] for the second order schemes without mass correction. The effective droplet radius thus becomes small and the oscillation frequency becomes large as shown in Fig. 2, since the frequency ω is given by the linear theory [6]:

$$\omega_n^2 = \frac{1}{We} \left[\frac{n(n-1)(n+1)(n+2)}{r_0^3(n+1+n\lambda)} \right], \quad (14)$$

where n , r_0 , and λ are the mode of oscillation, the average radius, and the density ratio, respectively. In our simulations, $n=2$, $r_0=1.0$, and $\lambda=0.01$. The mass correction is thus found to be necessary in our simulations to study nonlinear droplet oscillations quantitatively, and the distance and the mass corrections are both performed in the following.

It is noted here that reinitialization schemes may not be necessary if we use higher order numerical schemes and finer mesh systems for high resolution calculations [22]. However, this approach needs huge computational resources such as CPU time and memory size especially for three-dimensional simulations. Numerical efficiency is one of the important issues for the level set approach [18]. The distance and mass corrections described above are both very efficient, and few iterations are necessary [16,22]. In our simulations, the second order schemes are thus applied in time and space with the mass and distance corrections. It was also reported that reinitialization and mass correction were performed even for the extension velocity method [23], where the level set method was applied for the lattice Boltzmann method. It is also noted that the mass correction using Eq. (12) depends on the curvature. It was reported that the curvature in a level set framework was oscillatory [24]. Although the total mass is kept correctly in our simulations as shown in Fig. 3, the mass distribution may be affected by the curvature. The effect of curvature on the mass correction might be apparent in some flow problems.

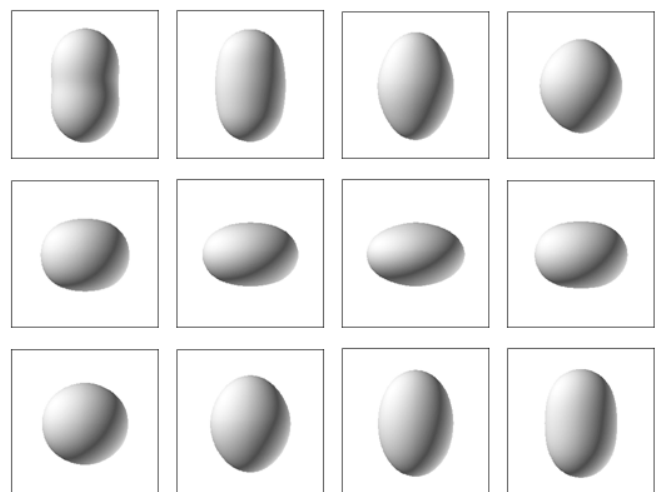


Fig. 4 Variation of droplet shape: $t=0.00, 0.99, 1.98, 2.96$ in the top row, $t=3.95, 4.95, 5.93, 6.92$ in the middle row, and $t=7.91, 8.89, 9.88, 10.87$ in the bottom row, from left to right.

B. Oscillations, Frequency and Damping

Variations of droplet shape during the first oscillation period are shown in Fig. 4 as examples of shape oscillations. The Reynolds number and the Weber number are 200 and 20, respectively, and the initial amplitude and the rotation rate are 0.38 and 0.0, respectively. The initial prolate shape given by the Legendre polynomial of order 2 becomes a spherical shape gradually, since the surface tension force is larger at the top and bottom poles. The droplet shape then becomes an oblate through the spherical shape, due to the inertia of internal flow. The surface tension force is larger at the equator for the oblate shape, and the droplet returns to a prolate shape again as shown in Fig. 4. The droplet shape varies dynamically due to the surface tension, and the oscillations between prolate and oblate shapes continue with some viscous damping.

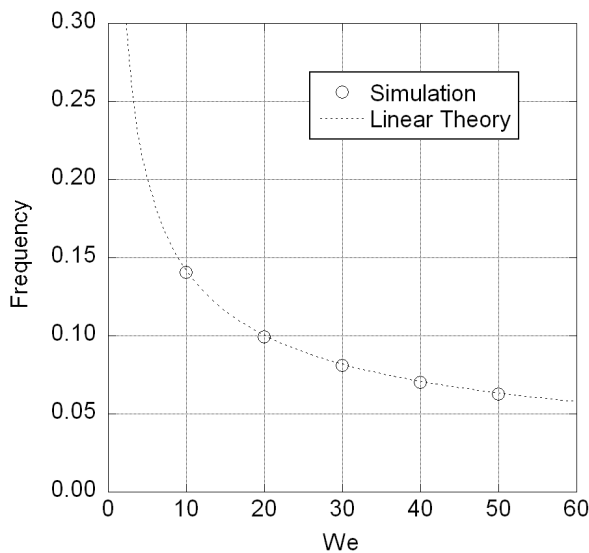


Fig. 5 Oscillation frequency as a function of surface tension.

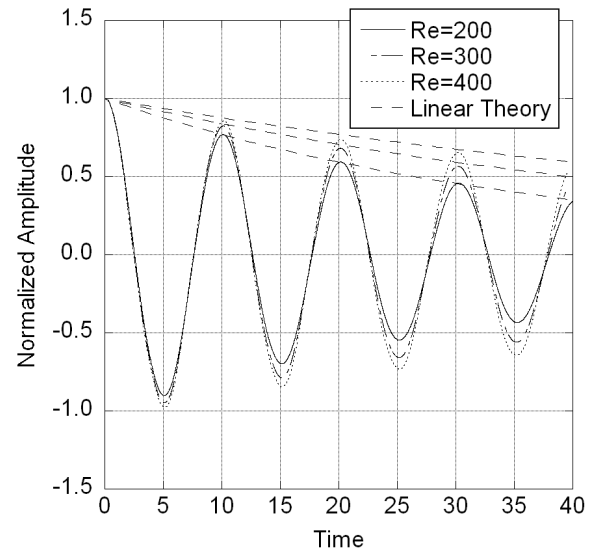


Fig. 6 Effects of viscosity on normalized amplitude.

The oscillation frequencies obtained using different surface tensions are compared in Fig. 5 with the theoretical value given by Eq. (14). The Reynolds number is fixed at 200, and the Weber number is varied. The initial amplitude is 0.02 so that the nonlinear effect of amplitude is small enough. It is shown that the agreement between the simulation and the linear theory is satisfactory. It is found that the present numerical simulations perform well for studying quantitatively the effect of the surface tension on the droplet oscillations.

Variations of normalized amplitude with different viscosity are shown in Fig. 6. The normalized amplitude is obtained as the oscillation amplitude normalized by the initial amplitude. It is shown that the damping is affected by the Reynolds number, while the oscillation frequency is almost the same. This is because the oscillation frequency depends on the surface tension as given by Eq. (14), and is not a function of viscosity. The effect of viscosity is estimated in terms of the damping constant. The oscillation amplitude is proportional to $\exp(-t/\tau)$, where the time constant τ is given by the linear theory [16],

$$\tau = \frac{r_0^2 \text{Re}}{(2n+1)} \left[\frac{n + \lambda(n+1)}{n(n+1) + \eta(n+1)(n+2)} \right]. \quad (15)$$

In the above equation, η is the viscosity ratio, which is 0.01 in our simulations. The damping of oscillation amplitude using Eq. (15) is shown in Fig. 6 for each Reynolds number. It is shown again that the agreement between the simulation and the linear theory is satisfactory. The present simulations are thus found to perform well for studying quantitatively the viscous effect as well.

It is confirmed so far that the effects of viscosity and surface tension, which are included in the nondimensional governing equations as the Reynolds number and the Weber number, respectively, are simulated quantitatively well in our simulations. This indicates that the reinitialization scheme using

Eqs. (9) and (12) is efficient for the level set approach to study the nonlinear droplet dynamics.

C. Effect of Amplitude on Oscillation Frequency

The effect of initial deformation on the time history of normalized amplitude is shown in Fig. 7. The Reynolds number and the Weber number are 200 and 20, respectively, and the rotation rate is 0.0. It is shown, as the amplitude increases, that the oscillation curves shift toward the positive direction of time axis and the frequency becomes small. The theoretical damping curve using Eq. (15) is also shown in Fig. 7. The agreement between the theoretical curve and the simulated results is not good for large amplitude, and it is found that the damping constant is also affected by the oscillation amplitude.

The relation between the oscillation frequency and the amplitude is shown in Fig. 8. It is shown clearly that the oscillation frequency decreases as the amplitude increases. The oscillation frequency is obtained by the linear theory in terms of the surface tension, density, radius and mode of oscillation as given by Eq. (14). The frequency is, however, shown to be affected much by the amplitude in Fig. 8. This is one of the important nonlinear characteristics of oscillating droplets known as the frequency shift [7-12]. The effect of mass correction is also indicated in Fig. 8. The result without mass correction shows higher frequencies, though the decrease in frequency is simulated qualitatively well. This is due to the decrease in droplet radius in Eq. (14) corresponding to the loss of mass shown in Fig. 3.

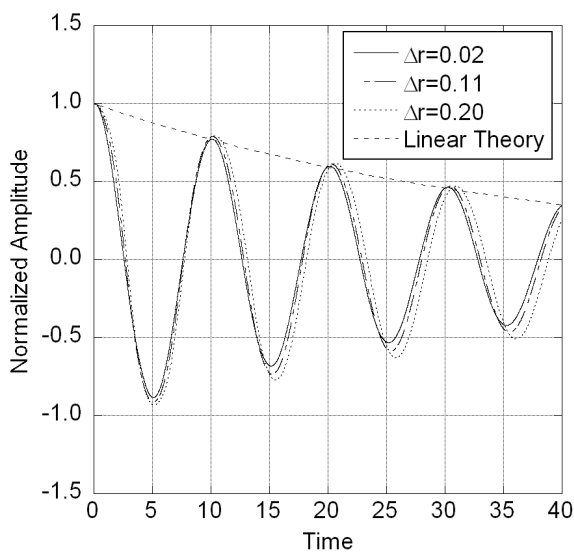


Fig. 7 Effect of initial deformation on normalized amplitude.

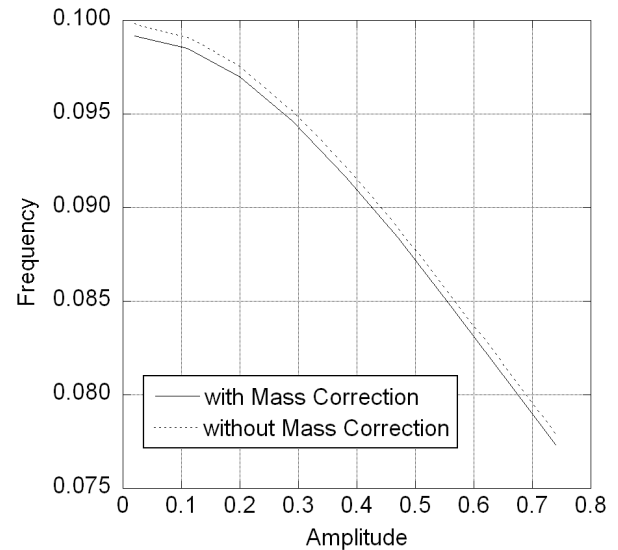


Fig. 8 Relation between frequency and amplitude: effect of mass correction.

The effects of surface tension and viscosity on the relation between the frequency shift and the oscillation amplitude are shown in Fig. 9. The vertical axis indicates the frequency shift, which is defined as the frequency difference normalized by the frequency for the amplitude of 0.02. The frequency itself decreases as the amplitude increases as shown in Fig. 8, and the frequency shift is thus negative and becomes large in Fig. 9. It is also shown that the frequency shift becomes large as the Reynolds number increases or the Weber number decreases, though these effects are not notable for small amplitude. The theoretical curve [13], which was derived by taking into account a second order deviation from the linear theory, is also shown along with the simulation results. The theoretical curve, in which the effects of surface tension and viscosity are not included, agrees well with the simulation result for small amplitude. It is found that the nonlinear effect due to the higher order deviation is notable, as well as the effects of viscosity and surface tension, as the oscillation amplitude becomes larger than 0.2.

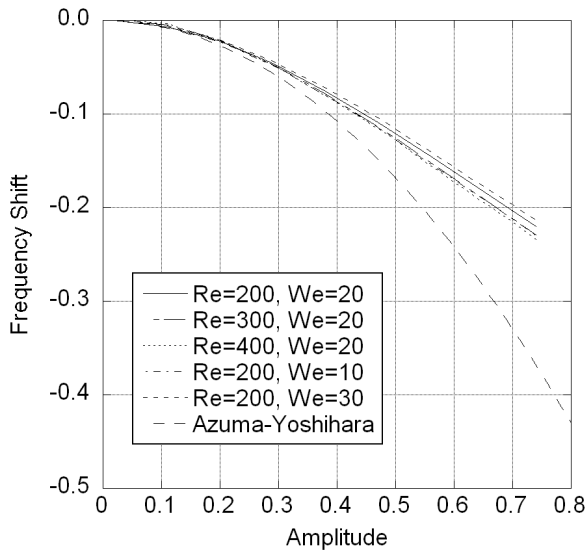


Fig. 9 Relation between frequency shift and amplitude: effects of surface tension and viscosity.

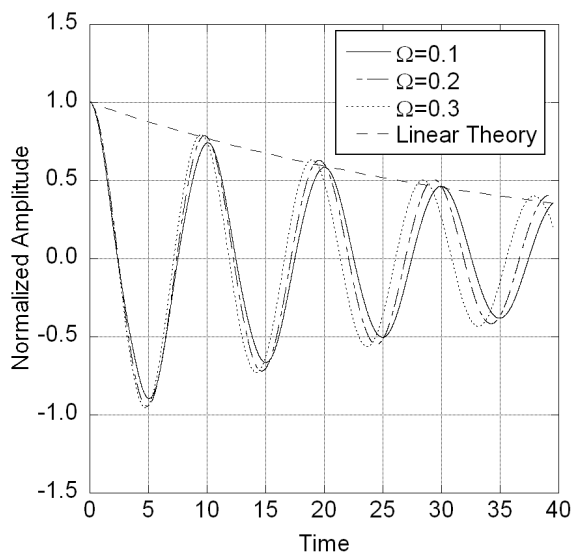


Fig. 10 Effect of rotation on normalized amplitude.

D. Effect of Rotation on Oscillation Frequency

The effect of rotation on the time history of normalized amplitude is shown in Fig. 10 for oscillations with the initial amplitude of 0.02. The Reynolds number is 200 and the Weber number is 20. In contrast to the effect of amplitude, the oscillation curves shift toward the negative direction of time axis and the frequency becomes large as the rotation rate increases. This is because the average force balance in the droplet is related to the oscillation frequency [25], and the centrifugal force provides the additional restoring force for oscillations of a rotating droplet [14]. The theoretical damping curve using Eq. (15) is also shown in Fig. 10. The agreement between the theoretical curve and the simulated results is not

good for large rotation rate, and the damping constant is also found to be affected by the rotation rate.

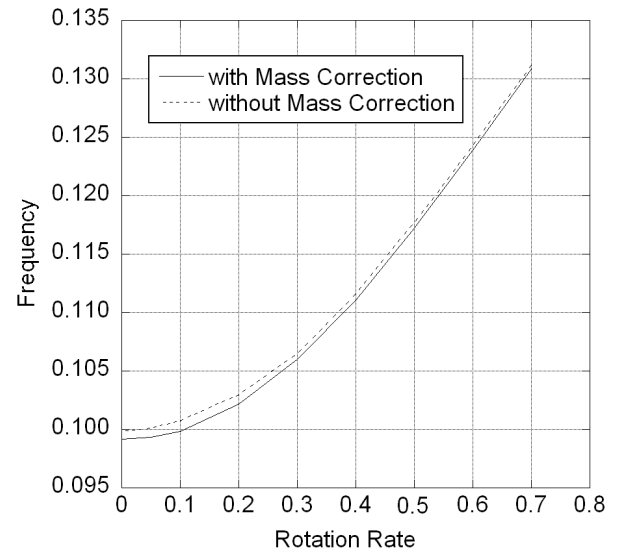


Fig. 11 Relation between frequency and rotation rate: effect of mass correction.

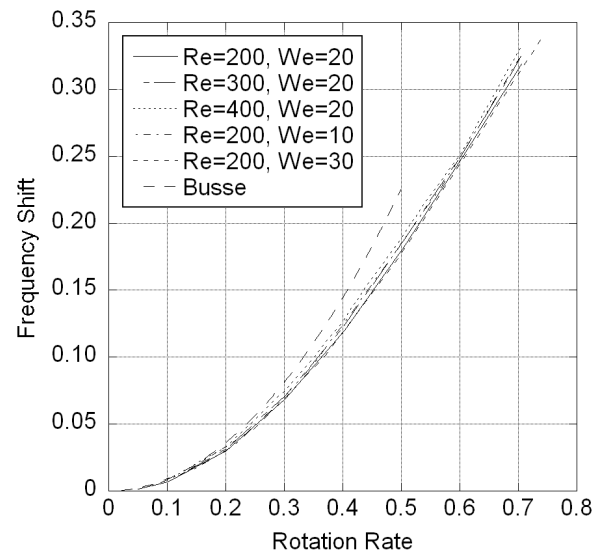


Fig.12 Relation between frequency shift and rotation rate: effects of surface tension and viscosity.

The relation between the oscillation frequency and the rotation rate is shown in Fig. 11. It is shown that the oscillation frequency increases as the rotation rate increases. The effect of mass correction is again indicated in Fig. 11. The result without mass correction shows slightly higher frequencies due to the loss of mass shown in Fig. 3. It is clear in Figs. 8 and 11 that the mass conservation is important for the level set approach to study the nonlinear droplet dynamics quantitatively.

The effects of surface tension and viscosity on the relation between the frequency shift and the rotation rate are shown in

Fig. 12. Although these effects are small, the frequency shift is shown to be large as the Reynolds number increases or the Weber number decreases as shown in Fig. 9. The theoretical curve [14], which was derived by taking into account a first order effect of the dynamic pressure due to rotation, is also shown along with the simulation results. The theoretical curve agrees well with the simulation results for small rotation rate. It is found that the nonlinear effect due to the higher order effect of rotation is notable, as well as the effects of viscosity and surface tension, as the rotation rate becomes larger than 0.2.

IV. CONCLUSION

In this study, nonlinear oscillations and rotations of a liquid droplet have been simulated numerically by solving the three-dimensional Navier-Stokes equations using the level set method. The importance of mass conservation was demonstrated, and the effective reinitialization scheme composed of mass and distance corrections was proposed. The frequency shifts due to the oscillation amplitude and the rotation rate, which are characteristic features of nonlinear droplet dynamics, were simulated well. It was shown that the simulated frequency shifts were in good agreement with the theoretical predictions for the normalized amplitude and the rotation rate smaller than 0.2. It was also shown that the effects of viscosity and surface tension on the frequency shift, which were not included in the theoretical predictions, were negligibly small as the normalized amplitude and the rotation rate were smaller than 0.2. The effects of nonlinearity, as well as the effects of viscosity and surface tension, became notable with increasing amplitude or rotation. It would be necessary for the theoretical treatments to include higher order terms with the effects of viscosity and surface tension for analyzing nonlinear droplet dynamics more precisely. Our approach using the level set method with accurate mass conservation would be applicable to simulations of complicated fluid phenomena involving two-phase interfaces [27] or free surfaces [28,29].

REFERENCES

- [1] S. Sauerland, G. Lohoefer, I. Egrý, Surface tension measurements on levitated aspherical liquid nickel drops, *Thermochimica Acta* 218, 1993, pp. 445-453.
- [2] I. Egrý, G. Lohoefer, G. Jacobs, Surface tension of liquid metals: results from measurements on ground and in space, *Phys. Rev. Lett.* 75, 1995, pp. 4043-4046.
- [3] M. Rosner-Kuhn, W. H. Hofmeister, G. Kuppermann, R. J. Bayuzick, M. G. Froberg, Investigations of the influence of oxygen on the surface tension of zirconium by the oscillating drop technique, *Surface Sci.* 443, 1999, pp. 159-164.
- [4] Y. Tian, R. G. Holt, R. E. Apfel, Investigation of liquid surface rheology of surfactant solutions by droplet shape oscillations: experiments, *J. Colloid and Interface Sci.* 187, 1997, pp. 1-10.
- [5] M. Przyborowski, T. Hibiya, M. Eguchi, I. Egrý, Surface tension measurement of molten silicon by the oscillating drop method using electromagnetic levitation, *J. Crystal Growth* 151, 1995, pp. 60-65.
- [6] H. Lamb, *Hydrodynamics*, sixth ed., Cambridge University Press, 1959.
- [7] E. Trinh, T.G. Wang, Large-amplitude free and driven drop-shape oscillations: experimental observations. *J. Fluid Mech.* 122, 1982, pp. 315-338.
- [8] E. Becker, W.J. Hiller, T.A. Kowalewski, Experimental and theoretical investigation of large-amplitude oscillations of liquid droplets. *J. Fluid Mech.* 231, 1991, pp. 189-210.
- [9] G. B. Foote, A numerical method for studying liquid drop behavior: simple oscillation, *J. comp. Phys.* 11, 1973, pp. 507-530.
- [10] J. A. Tsamopoulos, R. A. Brown, Nonlinear oscillations of inviscid drops and bubbles, *J. Fluid Mech.* 127, 1983, pp. 519-537.
- [11] T. W. Patzek, R. E. Benner Jr., O. A. Basaran, L. E. Scriven, Nonlinear oscillations of inviscid free drops, *J. comp. Phys.* 97, 1991, pp. 489-515.
- [12] O. N. Basaran, Nonlinear oscillations of viscous liquid drops, *J. Fluid Mech.* 241, 1992, pp. 169-198.
- [13] H. Azuma, S. Yoshihara, Three-dimensional large-amplitude drop oscillations: experiments and theoretical analysis. *J. Fluid Mech.* 393, 1999, pp. 309-332.
- [14] F. H. Busse, Oscillation of a rotating liquid drop. *J. Fluid Mech.*, 142, 1984, pp. 1-8.
- [15] T. Watanabe, Numerical simulation of oscillations and rotations of a free liquid droplet using the level set method, *Computers and Fluids* 37, 2008, pp. 91-98.
- [16] M. Sussman, P. Smereka, Axisymmetric free boundary problems, *J. Fluid Mech.* 341, 1997, pp. 269-294.
- [17] S. Osher, R. P. Fedkiw, Level set methods: an overview and some recent results, *J. Comp. Phys.* 169, 2001, pp. 463-502.
- [18] J. A. Sethian, P. Smereka, Level set methods for fluid interfaces, *Annu. Rev. Fluid Mech.* 35, 2003, pp. 341-372.
- [19] A.A. Amsden, F.H. Harlow, Simplified MAC technique for incompressible fluid flow calculations, *J. Comp. Phys.* 6, 1970, pp. 322-325.
- [20] T. Watanabe, Parallel computations of droplet oscillations, *Lecture Note in Computational Science and Engineering (LNCSE)* 67, 2009, pp. 163-170.
- [21] M. Sussman, P. Smereka, S. Osher, A level set approach for computing solutions to incompressible two-phase flow, *J. Comp. Phys.* 114, 1994, pp. 146-159.
- [22] Y.C. Chang, T.Y. Hou, B. Merriman, S. Osher, A level set formulation of Eulerian interface capturing methods for incompressible fluid flows. *J. Comp. Phys.* 124, 1996, pp. 449-464
- [23] C. Thommes, J. Becker, M. Junk, A.K. Vaikuntam, D. Kehrwald, A. Klar, K. Steiner, A. Wiegmann, A lattice Boltzmann method for immiscible multiphase flow simulations using the level set method. *J. Comp. Phys.* 228, 2009, pp. 1139-1156.
- [24] A. du Chene, C. Min, F. Gibou, Second-order accurate computation of curvatures in a level set framework using novel high-order reinitialization schemes, *J. Sci. Comput.* 35, 2008, pp. 114-131.
- [25] T. Watanabe, Zero frequency shift of an oscillating-rotating liquid droplet, *Phys. Lett. A* 372, 2008, pp. 482-485.
- [26] T. Watanabe, Flow field and oscillation frequency of a rotating liquid droplet, *WSEAS Trans. Fluid Mech.*, vol. 3, 2008, pp. 164-174.
- [27] N. M. S. Hassan, M. M. K. Khan and M. G. Rasul, Characteristics of air bubble rising in low concentration polymer solutions, *WSEAS Trans. Fluid Mech.*, Vol. 2, 2007, pp. 53-60.
- [28] M. DeMarchis and E. Napoli, 3D Numerical simulation of curved open channel flows, *WSEAS Trans. Fluid Mech.*, Vol. 1, 2006, pp. 175-180.
- [29] L. A. Mironova, O. I. Gubanov and S Kocabiyik, Numerical simulation of flow past an oscillating cylinder close to a free surface, *WSEAS Trans. Fluid Mech.*, Vol 1, 2006, pp. 297-303.

Tadashi Watanabe Ph. D. degree in Nuclear Engineering at Tokyo Institute of Technology, Japan, in 1985.

Research engineer in reactor safety division of Japan Atomic Energy Agency since 1985. The major research fields are nuclear reactor thermal hydraulics, reactor safety analysis, two-phase flow experiments and simulations, and computational science.

Member of Japan Atomic Energy Society, and Japan Mechanical Engineering Society.

watanabe.tadashi66@jaea.go.jp